HHS Public Access

Author manuscript

Kidney Int. Author manuscript; available in PMC 2018 October 01.

Published in final edited form as:

Kidney Int. 2017 October ; 92(4): 836–849. doi:10.1016/j.kint.2017.03.005.

Podocytes regulate the glomerular basement membrane protein nephronectin by means of miR-378a-3p in glomerular diseases

Janina Müller-Deile[1,2], **Jan Dannenberg**[1,2], **Patricia Schroder**[2], **Meei-Hua Lin**[3], **Jeffrey H.Miner**[3], **Rongjun Chen**[1], **Jan-Hinrich Bräsen**[4], **Thomas Thum**[5,6,7], **Jenny Nyström**[8], **Lynne Beverly Staggs**[2], **Hermann Haller**[1,2], **Jan Fielder**[5], **Johan M. Lorenzen**[1,5,7], and **Mario Schiffer**[1,2]

[1]Department of Medicine/Nephrology, Hannover Medical School, Hannover, Germany

[2]Mount Desert Island Biological Laboratory, Salisbury Cove, Maine, USA

[3]Division of Nephrology, Washington University School of Medicine, St. Louis, USA

[4]Department of Pathology, Hannover Medical School, Hannover, Germany

[5]Institute of Molecular and Translational Therapeutic Strategies, Hannover Medical School, Hannover, Germany

[6]Imperial College London, National Heart and Lung Institute, London, UK

[7]REBIRTH Excellence Cluster, Hannover Medical School, Hannover, Germany

[8]Department of Physiology and Department of Nephrology Sahlgrenska Academy, University of Gothenburg, Gothenburg, Sweden

Abstract

The pathophysiology of many proteinuric kidney diseases is poorly understood, and microRNAs (miRs) regulation of these diseases has been largely unexplored. Here, we tested whether miR-378a-3p is a novel regulator of glomerular diseases. MiR-378a-3p has two predicted targets relevant to glomerular function, the glomerular basement membrane matrix component, nephronectin (NPNT) and vascular endothelial growth factor VEGF-A. In zebrafish (Danio rerio), miR-378a-3p mimic injection or npnt knockdown by a morpholino oligomer caused an identical

Corresponding authors: Janina Müller-Deile, M.D., Mario Schiffer, M.D., Division of Nephrology, Hannover Medical School, Carl-Neuberg-Str. 1, 30625 Hannover, Germany, Phone++495115324708, FAX++49511552366, mueller-deile.janina@mh-hannover.de; schiffer.mario@mh-hannover.de.

Disclosure: None.

Ethics Statement: Zebrafish experiments were conducted according to the guidelines of the adherence to the NIH Guide for the Care and Use of Laboratory Animals and were approved by Institutional Animal Care and Use Committee of the Mount Desert Island Biological Laboratory, Maine (IACUC protocol#0804). All efforts were made to minimize the number of animals used and their suffering.

The approval for the mouse study was given by the ethical committee of Hannover Medical School and LAVES with the following number: 33.12-42502-04-14/1657.

Ethical approval was obtained from Ethics Committee of the Hanover Medical School (#1709-2013) for the use of urinary samples from patients with glomerular diseases for miR analysis.

phenotype consisting of edema, proteinuria, podocyte effacement and widening of the glomerular basement membrane in the lamina rara interna. Zebrafish vegf-A protein could not rescue this phenotype. However, mouse Npnt constructs containing a mutated 3′UTR region prevented the phenotype caused by miR-378a-3p mimic injection. Overexpression of miR-378a-3p in mice confirmed glomerular dysfunction in a mammalian model. Biopsies from patients with focal segmental glomerulosclerosis and membranous nephropathy had increased miR-378a-3p expression and reduced glomerular levels of NPNT. Thus, miR-378a-3p-mediated suppression of the glomerular matrix protein NPNT is a novel mechanism for proteinuria development in active glomerular diseases.

Keywords

Nephronectin; microRNA; membranous glomerulonephropathy; podocytes; glomerular basement membrane

Introduction

The glomerular filtration barrier is composed of three structural layers: the fenestrated endothelium, the glomerular basement membrane (GBM), and podocytes. Impairment of any single layer can have secondary effects on the other layers, ultimately leading to loss of function and proteinuria. In many cases, the initial cause of the disease and the functional interplay of GBM components during the disease process remain elusive.

MicroRNAs (miRs) regulate genes and are known to influence development, cell division, differentiation, and apoptosis (1). Therefore, they may be promising novel candidates in the study of glomerular diseases (2). Non-coding molecules 21 to 23 nucleotides in length, miRs bind the 3′-untranslated region (3′ UTR) of a target messenger RNA and inhibit translation (3). Those enriched in human kidneys include: miR-192, miR-194, miR-204, miR-215 and miR-216 (4). Furthermore, miRs are essential for podocyte homeostasis (5-8), and it was recently shown that focal segmental glomerulosclerosis (FSGS) induces the expression of miR-193a in podocytes (9). Moreover, miRs can be secreted in body fluids and therefore possibly could be biomarkers for various glomerular diseases (10, 11), potentially serving as early non-invasive diagnosis tools. Recently, *Kahai et al.* demonstrated that miR-378a-5p targets NPNT in osteoblasts (12). Nephronectin (NPNT) is an extracellular matrix protein localized in the GBM (13). However, the function and turnover of NPNT in the GBM is largely unexplored. After a common stress model for cultured human podocytes – TGF-β stimulation – we found miR-378a-3p upregulation. As -5p and -3p miRs of the same family often have the same targets (14-16), we speculated that miR-378a-3p would supress NPNT.

In this study, we show that miR-378a-3p supresses NPNT in zebrafish and murine models as well as in human glomerular diseases, and knockdown of NPNT leads to podocyte dysfunction and GBM disorganization. These findings accentuate the importance of podocyte/GBM interplay in glomerular disease.

Results

MiR-378a-3p is upregulated in stressed podocytes and targets NPNT

Transforming growth factor beta (TGF-β) is known to be important in the development of progressive podocyte diseases (17, 18). MiR-378a-3p was significantly upregulated in cultured human podocytes after TGF-β stimulation. This increase was time dependent ($p < 0.01$, Fig. 1A). On the other hand, miR-378a-5p expression was not altered by TGF-β (data not shown). Nevertheless, TGF-β stimulation decreased both NPNT protein and mRNA expression in cultured human podocytes in a time-dependent manner. This decrease was directly inverse to the miR-378a-3p increase (Fig. 1B-C). Furthermore, NPNT mRNA expression was significantly higher in cultured human podocytes compared to other glomerular cell types ($p < 0.01$ Fig. 1D). To further analyse the potential interaction between miR-378a-3p and NPNT, podocytes were transfected with pre-miR-378a-3p oligonucleotide (miR-378a-3p mimic). This led to suppression of NPNT protein (Fig. 1E, supplementary Fig. 1) compared to control. In contrast, transfection of cultured human podocytes with a chemically modified, single-stranded oligonucleotide that bind and inhibit miR-378a-3p (miR-378a-3p inhibitor) increased NPNT mRNA. However, when used in the presence of TGF-β, the miR-378a-3p inhibitor had no effect on NPNT mRNA (Fig. 1F), suggesting that TGF-β also suppresses NPNT by a mechanism independent of miR-378a-3p.

Nevertheless, online target prediction tools (mirtarbase, FindTar3) identified NPNT as a potential target of miR-378a-3p. The binding site for miR-378a-3p on the NPNT mRNA is conserved across zebrafish, mice and human (supplementary Fig. 2A). FindTar3 prediction tool calculated free energy no greater than -20.9 kcal/mol and central loop score of 25 for the binding of miR-378a-3p to the NPNT 3′-UTR. According to the assessing criteria for target predicted by FindTar3 based on central loop score and free energy, this binding was excellent.

MiR-378a-3p is conserved across species but the 3′-UTRs of NPNT is species specific. The miR-378a-3p binding locus is, nevertheless, conserved on the 3′-UTR of all species (supplementary Fig. 2A). With the cloning of wildtype human NPNT 3′-UTR to a luciferase reporter construct we now could emphasize that miR-378a-3p directly targets NPNT-3′-UTR (Fig. 1G).

Both morpholino npnt knockdown and miR-378a-3p mimic injection cause loss of plasma proteins in zebrafish

To investigate the relevance of miR-378-3p, and its target NPNT, *in vivo*, we used the model organism zebrafish (*Danio rerio*). Human NPNT and zebrafish npnt have 77 % amino acid sequence homology and a conservation of functional domain structure (supplementary Fig. 2B). Injection of a npnt-specific morpholino (npnt-MO) or a miR-378a-3p-mimic in 1-4 cell stage zebrafish larvae significantly decreased npnt mRNA (supplementary Fig. 3). Zebrafish with less npnt had pericardial edema and yolk sac edema. We classified the resulting phenotypes with a previously described method. In short, phenotypes ranged from phenotype 1 (P1) – no edema – to phenotype 4 (P4) – severe edema (19). 57 % of npnt-MO

injected and 42 % of the miR-378a-3p injected larvae developed severe edema, whereas CTRL-MO and miR-CTRL injected embryos mostly had no edema (Fig. 2A, left).

To test for protein leakage through the glomerular filter, we used transgenic zebrafish that expresses a 78 kDa Vitamin D binding protein tagged with enhanced green fluorescent protein (EGFP) (Tg(l-fabp:DBP:EGFP) (19). Loss of EGFP, quantified over the retinal vessel plexus, indicates loss plasma proteins through glomerular leakage (20, 21).

Both npnt-MO and miR-378a-3p mimic injected zebrafish larvae displayed significantly less EGFP in the retinal vessel plexus compared to respective controls at 96 hours post fertilization (hpf) ($p< 0.001$, Fig. 2A, right panel).

To rule out that the observed phenotype was due to a disruption of glomerular development, we used a separate zebrafish model. During normal zebrafish kidney development, the two filter units of the pronephros fuse at 48 hpf. At this time, development is complete and the glomerulus is fully functional. Examination of transgenic zebrafish that express the glomerular-specific Wilms tumor 1b protein linked to EGFP (wt1b:EGFP zebrafish) (19) revealed proper pronephric fusion at 48 hpf in all examined conditions (supplementary Fig. 4).

In addition, fish injected with miR-378a-3p mimic at 48 hpf also developed an edematous phenotype, albeit less severe than fish injected as 1-4 cell stage egg (Fig. 2B). Interestingly, no significant plasma protein loss was detectable in miR-378a-3p mimic injected embryos at 96 hpf. At 120 hpf, however, miR-378a-3p mimic injected zebrafish developed significant proteinuria (Fig. 2B).

To rule out the possibility that loss of fluorescence was caused by miR or MO interference with EGFP expression and further confirm a permeability defect of the glomerular filtration barrier, we injected fluorescent dextrans of different molecular weights in wildtype zebrafish larvae at 72 hpf. MiR-378a-3p and npnt-MO injected larvae had quantifiably less 70 kDa dextrans in the retinal vessel plexus. This loss was comparable to that of EGFP tagged Vitamin D binding protein in previous experiments. Moreover, high sensitivity protein electrophoresis detected 70 kDa dextran in the water of both miR-378a-3p and npnt-MO injected zebrafish larvae, while no 70 kDa dextran was detected in water of control larvae (Fig. 2C).

In contrast, miR-378a-3p mimic and npnt-MO injection had no effect on 2000 kDa dextrans levels (supplementary Fig. 5), showing that protein loss was due to glomerular leakage and not unspecific vascular leakage.

Both npnt-MO and miR-378a-3p mimic injection induce podocyte foot process effacement and GBM changes in zebrafish

To determine which layer of the glomerular filtration barrier was affected by npnt-MO or miR-378a-3p mimic, we performed transmission electron microscopy (TEM) on glomeruli at 120 hpf. Podocyte foot processes were scored as normal, partially effaced or completely effaced. Both miR-378a-3p and npnt-MO injection resulted in increase in podocyte effacement compared to controls (Fig. 3A).

Ultrastructural changes of the GBM were also observed in both miR-378a-3p mimic and npnt-MO injected larvae, the most prominent of which were massive widening and disintegration of the space to the glomerular endothelium in the lamina rara interna. Morphology of the glomerular lamina rara externa and lamina densa of miR-378a-3p mimic or npnt-MO injected larvae was comparable to controls (Fig. 3B).

Vegf-Aa does not rescue miR-378a-3p induced glomerular damage

The second prominent target of miR-378a-3p with a potential role for glomerular structure and function is vegf-Aa. To test the hypothesis that miR-378a-3p suppression of npnt caused the previously shown glomerular phenotype, we targeted vegf-Aa using a morpholino. Vegf-Aa knockdown by a splice donor morpholino (vegf-Aa-MO) caused a phenotype with proteinuria and edema similar to the observed phenotype after both npnt-MO and miR-378a-3p injections (Fig. 4A, B). However, on the ultrastructural level, the glomerular damage was completely different from the damage seen after miR-378a-3p mimic injection in zebrafish larvae. The prominent structural changes after vegf-Aa-MO injection were swelling and thickening of glomerular endothelial cells, a phenotype resembling changes seen in preeclampic mammals. Although podocyte effacement was detectable in some areas, the predominant GBM phenotype of both npnt-MO and miR-378a-3p mimic injected fish was not present (Fig. 4C).

To further rule out involvement of vegf-Aa in the miR-378a-3p induced phenotype, we performed rescue experiments with co-injections of recombinant zebrafish vegf-Aa protein. To adjust dosage and test the rescue, we injected vegf-Aa-MO together with zebrafish recombinant vegf-Aa protein.

Recombinant vegf-Aa rescued proteinuria, edema and structural glomerular damage caused by vegf-Aa-MO, but when injected together with miR-378a-3p mimic, recombinant vegf-Aa had no effect on proteinuria, podocyte effacement or GBM thickening (Fig. 4A-C). Thus, miR-378a-3p suppression of npnt, and not vegf-Aa, was responsible for the observed phenotype.

Crosspieces rescue with different mouse Npnt constructs after miR-378a-3p mimic injection in zebrafish

To confirm, that miR-378a-3p downregulates npnt in zebrafish by binding to the 3′UTR region, we did transspecies rescue experiments using different mouse Npnt constructs: One construct contained the functional domains of Npnt together with the wildtype 3′UTR region (Npnt+3′). The second construct contained the functional domains of Npnt together with a mutant 3′UTR region designed to prevent miR-378a-3p seed region binding (Npnt +mu3′). Transfection of HEK cells with mouse Npnt+3′ construct or Npnt+mu3′ construct confirmed expression of Npnt protein (supplementary Fig. 6).

83 % of zebrafish injected with miR-378a-3p mimic alone and 84 % of zebrafish injected with both miR-378a-3p mimic and Npnt+3′ construct (miR-378a + Npnt+3′) developed edema with P3 or P4 phenotype. Loss of plasma proteins was also comparable between both groups, indicating that the miR-mimic not only binds to the zebrafish npnt but also to the injected cRNA. Injection of both miR-378a-3p mimic and mouse Npnt+mu3′ construct

(miR-378a + Npnt+mu3′) however rescues phenotype and loss of plasma proteins caused by miR-378a-3p. Only 34 % of zebrafish developed P3 or P4 phenotype whereas the rest developed normal (Fig. 5A, B).

MiR-378a-3p mimic injection leads to albuminuria, podocyte effacement and altered expression of podocyte proteins in mice

In order to validate our findings in a mammalian model, 6-week-old mice received serial i.p injections of miR-378a-3p mimic or control miR at days 1, 3, 7, and 14. Urine samples were collected for analysis weekly. 21 days after the first miR-378a-3p mimic injection, mice had developed detectable albuminuria (Fig. 6A) and displayed an increased urine protein creatinine ratio (UPC-ratio, Fig. 6B). Serum creatinine and urea of miR-378a-3p mimic injected mice, however, remained comparable to controls (Fig. 6C, D). Real-time PCR, western blot of whole kidney, and immunofluorescent staining revealed significantly less Npnt in miR-378a-3p mimic injected mice than in control mice 28 days after initial injection (Fig. 6E-G).

To investigate glomerular Npnt expression in mice we performed co-staining with agrin, a major heparan sulfate proteoglycan of the GBM. Npnt was localized in a GBM-like pattern that showed a partial overlap with agrin (Fig. 6H).

Other GBM proteins such as collagen α 345(IV) (Col4A345) were expressed in the GBM of miR-378a-3p injected mice at levels comparable to controls. Interestingly, podocin was redistributed in a speckled expression pattern in miR-378a-3p mimic injected mice compared to homogenous staining in control mice (Fig. 6H, D-I).

TEM images of mice injected with miR-378a-3p mimic displayed foot process effacement comparable with effacement observed in miR-378a-3p mimic-injected zebrafish. In contrast, the changes detected in GBM architecture of miR-378a-3p mimic injection in zebrafish could not be confirmed in mice. No phenotypes were observed in controls (Fig. 6I).

MiR-378a-3p and NPNT expression are altered in human glomerular diseases

To characterize the glomerular expression pattern of NPNT in humans, healthy human kidney cortex sections were stained with immunofluorescent antibodies.

NPNT co-localized with collagen IV and podocalyxin, indicating predominant expression in podocytes and the GBM (Fig. 7A).

Next, we examined expression patterns of miR-378a-3p and NPNT in kidney biopsy samples of patients with different glomerular diseases. In-situ hybridization detected more miR-378a-3p expression in glomeruli with idiopathic membranous glomerulonephritis (iMGN) ($p < 0.05$) and FSGS ($p < 0.05$) than compared healthy control tissue. In patients with minimal change disease (MCD) and IgA glomerulonephritis (IgA-GN) no changes were detected. Contrary to expectations, cells of diabetic nephropathy (DN) patients expressed less miR-378a-3p than healthy controls ($p < 0.001$) (Fig. 7B).

In line with a proposed regulation of NPNT by miR-378a-3p, we found less expression of NPNT in glomeruli of patients with iMGN ($p< 0.001$) and FSGS ($p< 0.05$) compared to healthy controls. MCD and IgA-GN did not change NPNT expression. In biopsies from patients with DN, NPNT stained strongly in glomeruli with extended matrix accumulations ($p<0.001$ compared to controls) (Fig. 7C) but weakly in glomeruli that appeared healthy (data not shown).

Analysis of pooled urines revealed significant miR-378a-3p upregulation in patients with iMGN, FSGS and MCD, but no changes were found in urines from patients with other glomerular diseases (supplementary Fig. 7).

Discussion

Proper filter function requires a coordinated interplay among extracellular structures, circulating factors, and the different cell types and layers of the glomerular filtration barrier. Dysfunction in any layer of the glomerular filtration barrier may lead to proteinuria. As podocytes and glomerular endothelial cells constantly add matrix components to the GBM, impairment of either can result in altered GBM composition. Under normal conditions, podocytes add and assemble collagen IV, laminin, fibronectin and proteoglycans to the GBM (22). Yet, communication is not unidirectional. Abnormalities in the GBM may cause matrix-to-cell signalling impairments that affect surrounding podocytes, mesangial cells and endothelial cells (23). However, because podocyte foot processes directly attach to the GBM, interactions between podocytes and the GBM seem to be of special importance. Mutations in collagen IV cause Alport syndrome, which is associated with a disrupted GBM and proteinuria (24, 25). Similarly, loss or missense mutations in the laminin-β-2 (LAMB2) gene cause nephrotic syndrome in Pierson syndrome and lead to podocyte distress and injury (26-28). The significance of podocyte-GBM interactions also apply to other glomerular diseases. In iMGN, the GBM is thickened due to the accumulation of GBM matrix between and around subepithelial immune complex deposits (29). Integrin-α-2 knockout mice develop proteinuria and irregular thickening and protrusions of the GBM by 5 months of age (30). Conditional loss of laminin-α-5 in podocytes results in proteinuria, progressive GBM thickening, and podocyte foot process effacement (31).

In recent years, miRs were shown to regulate extracellular matrix proteins (32). However, the extent to which miRs alter podocyte extracellular matrix production in glomerular disease is unknown.

Here we describe miR-378a-3p, a novel regulator of podocyte-derived extracellular matrix protein NPNT/Npnt/npnt. MiRs mediate gene regulation through binding 3′-UTRs of target mRNAs. After pairing the miR and mRNA incorporate into a silencing complex, leading to post-transcriptional repression by either mRNA degradation, translational repression, or both (33). MiR target databases (birtarbase, FINDTAR3, starbase) consistently predicated NPNT as a target of miR-378a-3p.

We verified that miR-378a-3p suppresses NPNT/npnt/Npnt expression, most likely by RNA degradation, in human podocytes, zebrafish and mice. Similar finding in osteoblasts confirm NPNT as a bona fide target of miR-378a-3p (34).

NPNT is an extracellular matrix protein and reported ligand of integrin α8-β1 during kidney development (35-37). Mass spectrometry proteomics and correlation intensity analysis of glomerular extracellular matrix fractions localize NPNT to the GBM (13). However, the function and turnover of NPNT in the GBM is unclear.

In our findings, NPNT was regulated through TGF-β in cultured human podocytes, shown by real time PCR, immunofluorescent staining and western blot. TGF-β plays a role in progressive podocyte diseases, such as FSGS (38) and iMGN (39, 40). Furthermore, TGF-β protein is increased along glomerular capillary walls and in the urine in iMGN (41, 42). In line with our results, downregulation of NPNT by TGF-β has been shown in osteoblasts (43, 34). However, our miR-378a-3p inhibitor experiments in cultured human podocytes suggest that TGF-β also regulates NPNT independent of miR-378a-3p.

The zebrafish pronephros consists of a single glomerulus that is structurally very similar to its human counterpart and can therefore serve as an experimental model of glomerular diseases (44). Fluorescent dextran injection experiments demonstrate that the zebrafish glomerular filtration barrier is already developed at around 48 hpf (45). npnt knockdown in zebrafish larvae by either injection of npnt-MO or miR-378a mimic resulted in generalised edema, and detection of injected 70 kDa fluorescence-labelled dextran in the water indicated proteinuria. These phenotypes could also be induced at 48 hpf, after pronephros development and midline fusion is completed. Thus, a delay in renal developmental due to miR-378a-3p expression or npnt-MO was excluded as the cause of the detrimental phenotype. Rather, podocyte effacement, together with the thickening of the GBM, was identified as the ultrastructural cause of proteinuria. Interestingly, the lamina rara interna was specifically disfigured in both npnt-MO and miR-378a-3p mimic injected zebrafish. The lamina rara externa and lamina densa of the GBM were intact.

npnt-MO and the miR-378a-3p mimic injection caused comparable phenotypes. This is most likely due to miR-378a-3p targeting of npnt. Other predicted target mRNAs of miR-378a-3p/-5p such as SUFU and TOB2 (46-48) are relevant to oncogenic transformation but are not described as relevant in kidney cells or disease. In contrast, VEGF-Aa is another target of miR-378a-3p with an important glomerular barrier function, but this is restricted to glomerular endotheliosis (49). The injection of recombinant zebrafish vegf-Aa protein was able to rescue the phenotype caused by vegf-Aa-MO but not the phenotype caused by miR-378a-3p mimic injection, thereby excluding miR-378a-3p targeting of VEGF-Aa as a cause of the glomerular phenotype.

To further confirm the effect of miR-378a-3p on npnt, we used to two different mouse Npnt constructs: a Npnt+3′ construct containing the functional domains of Npnt together with the 3′UTR region and a Npnt+mu3′ construct containing the functional domains of Npnt together with a mutation the 3′UTR region so that the miR could not bind. The cRNA of the Npnt+mu3′ construct was able to prevent proteinuria and edema due to miR-378a-3p mimic

injection. In contrast, when miR-378a-3p mimic was injected together with the cRNA of Npnt+3′ construct, zebrafish still developed edema and loss of plasma proteins indicating that the miR-mimic not only bound to the zebrafish npnt but also to the injected cRNA for Npnt.

We confirmed the pathological role of miR-378a-3p in a mammalian model. MiR-378a-3p mimic injection caused albuminuria by altering GBM proteins and effacing podocyte foot processes in mice.

MiR-378a-3p mimic injection significantly altered podocin expression but left Col4A345 unchanged. The GBM phenotype seen is zebrafish larvae, however, could not be reproduced in mice. This may be explained by a higher sensitivity of zebrafish larvae, which is dependent on a single pronephros, compared with a mammalian system that has many glomeruli

In humans, miR-378a-3p was expressed in podocytes under healthy conditions. This expression was increased in patients with iMGN and FSGS. NPNT staining in healthy conditions revealed a pattern following GBM structure that co-localized with collagen IV and podocyalyxin in the glomerulus. However, in iMGN and FSGS glomerular NPNT expression was significantly decreased.

We were not the first to explore NPNT expression in human glomerular diseases. *Nakatani et al* previously showed increased NPNT deposition in DN, which is in line with our findings, but they noted no changes in NPNT expression in FSGS and MCD (50, 51). However, this group used a different NPNT antibody.

Our clinical findings indicate that both altered NPNT and miR-378a-3p expression may play a role in different human glomerular diseases. To investigate if miR-378a-3p might serve as a biomarker, we measured miR-378a-3p in urine samples from patients with different glomerular diseases. MiR-378a-3p was more concentrated in urine samples of patients with FSGS, iMGN and MCD than healthy controls and other glomerular diseases. MiR-378a-3p in the urine might therefore have the potential as a non-invasive biomarker for glomerular damage.

In summary, miR-378a-3p mediated suppression of NPNT expression may be a novel mechanistic pathway in glomerular diseases. To our knowledge, this is the first description of cell-matrix crosstalk via miRs in glomerular cells. Impairments in NPNT expression can lead to podocyte damage and alteration of the GBM. Thus, miR-378a-3p may be a non-invasive diagnostic marker or a potential target for treatment of glomerular diseases.

Materials and methods

Cell culture

A detailed description can be found in the supplements.

Urine sample preparation for miR analysis

A detailed description can be found in the supplements. Ethical approval was obtained from Ethics Committee of the Hanover Medical School (#1709-2013).

MiR real-rime PCR in urines and cells and mRNA real-time PCR in cells and organ tissue lysates

Protocols can be found in supplements

Luciferase assay and target prediction

A detailed description can be found in the supplements.

Transfection of miR mimics in podocytes

We used the mirVana® miRNA mimic has-miR-378a-3p (miR-378a-3p mimic, Life Technologies, Carlsbad, CA) and mimic and miRVana miR-negative control (miR-CTRL, Life Technologies, Carlsbad, CA) for cell culture experiments in human podocytes. Cultured human podocytes were transfected with 2 μl/ml miR-378a-3p mimic/ miR-CTRL for 4 h using Lipofectamin and Opti-MEM Medium (Thermo Fisher scientific, Waltham, MA) according to manufactures protocol.

Western Blotting

Protocols can be found in supplements.

In-situ-hybridization of miRs

MiRCURY LNA™ microRNA ISH Optimization Kit (Exiqon, Vedbaek, Denmark) was used to perform in situ hybridization on paraffin embedded kidney biopsies according to the manufacturer's protocol. Double 3′ and 5′ DIG labelled MiRCURY LNA™ Detection probes for miR-378a-3p (GCCTTCTGACTCCAAGTCCAGT) were used. Hybridization temperature was 55° C for 1 h.

In vivo studies in zebrafish

Zebrafish were grown and mated at 28.5° C. Larvae were kept and handled in standard E3 solution as previously described (52). Injection of npnt-MO (100 μM), MO-CTRL (100 μM), miR-CTRL (25 μM, mirVana® miRNA mimic, negative control; Life Technologies, Carlsbad, lCA) and miR-378a-3p mimic (25 μM, mirVana® miRNA mimic, has-miR-378a-3p; Life Technologies Carsbad, CA) into zebrafish eggs at one to four cell stage was performed as previously described (19). Morpholinos were ordered from Gene Tools (Philomath, OR) (sequences in supplementary table 1). For 48 hpf injection, zebrafish larvae were anesthetized with tricaine and injected with a 50 μM miR-378a-3p mimic or a miR-CTRL through the cadinal vein. For measurement of glomerular filter integrity, transgenic zebrafish that expresses a GFP tagged Vitamin D binding protein (*Tg(l-fabp:DBP:EGFP) fish*) were used as previously described (19, 52). The maximum fluorescence intensities of grayscale images of the pupil of the fish were measured using Image J (Version 1.48 Wayne Rasband National Institutes of Health, USA) and reported in relative units of brightness. A second transgenic zebrafish strain that expresses a green fluorescent Wt1b (wt1b:eGFP

zebrafish) was used to monitor proper glomerular fusion during zebrafish development (19). The Mount Desert Island Biological Laboratory (MDIBL) animal care committee approved the animal protocol (IACUC protocol #0804).

npnt rescue in zebrafish with mouse Npnt constructs

Npnt+3′ DNA construct and Npnt+mu3′ DNA construct (kind gifts from Burton B. Yang) have been previously published (13). From these constructs capped RNAs were synthesized using mMESSAGE mMACHINE® kits (Ambion, Life Technologies, Carsbad, CA) according to manufacturer's protocol. Since capped RNA (cRNA) has a 7-methyl guanosine cap structure at the 5′ end, it mimics most eukaryotic mRNAs found *in vivo*.

Using the Nanoject II injection device (Drummond Scientific, Broomall, PA), 4.6 nl cRNA of Npnt+3′construct a.e. 4.6 nl cRNA of Npnt+mu3′ were injected together with miR-378a-3p mimic into one to four-cell stage fertilized zebrafish larvae.

Transmission electron microscopy of zebrafish glomeruli

Zebrafish larvae were fixed at 120 hpf in solution D and embedded in EPON (recipe/ protocol from EMS, Hatfield, PA). Semi-thin (300 nm) and ultra-thin (90 nm) sectioning were performed with a Leica UC-6 Microtome and transferred onto copper slit grids (EMS, Hatfield, PA). Grids were stained with uranyl acetate (2 %) for 30 min and then lead citrate for 15 min with three washing steps in between. Imaging was done with a JOEL JEM-1230 transmission electron microscopy. The podocyte layer was analysed over a length of 91 μm for WT, 98 μm for miR-378a-3p, 86 μm for miR-CTRL, 104 μm for npnt-MO, 80 μm for CTRL-MO, 78 μm for c.v. miR-378a-3p and 84 μm for c.v. miR-CTRL.

Injection of miR mimics in mice

6 weeks old CD1 mice (Crl:CD1 (ICR),Charles River, Wilmington, MA) were i.v. injected with miR-CTRL (0.2 mg/ mouse, mirVana® miRNA Mimic, Negative Control; Life Technologies, Carlsbad, CA) or miR-378a-3p mimic (0.2 mg/ mouse, mirVana® miRNA mimic, has-miR-378a-3p; Life Technologies, Carlsbad, CA) at day 0, 3, 7 and 14. At baseline, day 7, 14, 21 and 28 serum samples were collected from tail vein and urine samples were collected by putting the mice in metabolic cages over 24 h. Mice were sacrificed at day 28 and kidneys were harvested for electron microscopy, protein, cryo sectioning and RNA.

Data analysis/ statistics

We used the delta-delta cycle threshold (CT) method to normalize PCR data and to generate fold changes in miR expression. The fold change is the relative quantitative value calculated by $2^{-(\text{delta-delta CT})}$. Delta-delta CT = delta CT (sample) – delta C (reference) with delta C (sample) = CT value for sample normalized to endogenous housekeeping gene and delta CT (reference) = CT value for calibrator normalized to endogenous housekeeping gene. Housekeeper were U6 for cells in miR PCRs, cel-39 for urine in miR PCR and GAPDH in mRNA PCRs.

All data are shown as means ± SD and were compared by ANOVA to look for statistical significance.

Supplementary Material

Refer to Web version on PubMed Central for supplementary material.

Acknowledgments

We thank Burton B.Yang for his kind gifts of the Npnt+mu3′UTR and Npnt+3′UTR constructs, and Nathan D Susnik for scientific and English language editing of this manuscript.

References

1. Bushati N, Cohen SM. MicroRNA functions. Annu Rev Cell Dev Biol. 2007; 23:175–205. DOI: 10.1146/annurev.cellbio.23.090506.123406 [PubMed: 17506695]
2. He L, Hannon GJ. MicroRNAs: Small RNAs with a big role in gene regulation. Nat Rev Genet. 2004; 5(7):522–531. DOI: 10.1038/nrg1379 [PubMed: 15211354]
3. Denli AM, Tops BB, Plasterk RH, et al. Processing of primary microRNAs by the microprocessor complex. Nature. 2004; 432(7014):231–235. DOI: 10.1038/nature03049 [PubMed: 15531879]
4. Sun Y, Koo S, White N, et al. Development of a micro-array to detect human and mouse microRNAs and characterization of expression in human organs. Nucleic Acids Res. 2004; 32(22):e188.doi: 10.1093/nar/gnh186 [PubMed: 15616155]
5. Wu J, Zheng C, Fan Y, et al. Downregulation of MicroRNA-30 facilitates podocyte injury and is prevented by glucocorticoids. J Am Soc Nephrol. 2013; 25(1):92–104. DOI: 10.1681/ASN.2012111101 [PubMed: 24029422]
6. Zhdanova O, Srivastava S, Di L, et al. The inducible deletion of drosha and microRNAs in mature podocytes results in a collapsing glomerulopathy. Kidney Int. 2011; 80(7):719–30. DOI: 10.1038/ki.2011 [PubMed: 21544061]
7. Harvey SJ, Jarad G, Cunningham J, et al. Podocyte-specific deletion of dicer alters cytoskeletal dynamics and causes glomerular disease. J Am Soc Nephrol. 2008; 19(11):2150–8. DOI: 10.1681/ASN.2008020233 [PubMed: 18776121]
8. Li D, Lu Z, Jia J, et al. Changes in microRNAs associated with podocytic adhesion damage under mechanical stress. J Renin Angiotensin Aldosterone Syst. 2013; 14(2):97–102. DOI: 10.1177/1470320312460071 [PubMed: 23087255]
9. Gebeshuber CA, Kornauth C, Dong L, et al. Focal segmental glomerulosclerosis is induced by microRNA-193a and its downregulation of WT1. Nat Med. 2013; 19(4):481–487. DOI: 10.1038/nm.3142 [PubMed: 23502960]
10. Wang N, Zhou Y, Jiang L, et al. Urinary microRNA-10a and microRNA-30d serve as novel, sensitive and specific biomarkers for kidney injury. PLoS One. 2012; 7(12):e51140.doi: 10.1371/journal.pone.0051140 [PubMed: 23272089]
11. Wang G, Kwan BC, Lai FM, et al. Expression of microRNAs in the urinary sediment of patients with IgA nephropathy. Dis Markers. 2010; 28(2):79–86. DOI: 10.3233/DMA-2010-0687 [PubMed: 20364043]
12. Kahai S, Lee SC, Lee DY, et al. MicroRNA miR378 regulates nephronectin expression modulating osteoblast differentiation by targeting GalNT-7. PLoS One. 2009; 4(10):e7535.doi: 10.1371/journal.pone.0007535 [PubMed: 19844573]
13. Lennon R, Byron A, Humphries JD, et al. Global analysis reveals the complexity of the human glomerular extracellular matrix. J Am Soc Nephrol. 2014; 25(5):939–951. DOI: 10.1681/ASN.2013030233 [PubMed: 24436468]
14. Almeida MI, Nicoloso MS, Zeng L, et al. Strand-specific miR-28-5p and miR-28-3p have distinct effects in colorectal cancer cells. Gastroenterology. 2012; 142(4):886–896.e9. DOI: 10.1053/j.gastro.2011.12.047 [PubMed: 22240480]

15. Patnaik SK, Kannisto E, Mallick R, et al. Overexpression of the lung cancer-prognostic miR-146b microRNAs has a minimal and negative effect on the malignant phenotype of A549 lung cancer cells. PLoS One. 2011; 6(7):e22379.doi: 10.1371/journal.pone.0022379 [PubMed: 21789255]
16. Jiang L, Huang Q, Zhang S, et al. Hsa-miR-125a-3p and hsa-miR-125a-5p are downregulated in non-small cell lung cancer and have inverse effects on invasion and migration of lung cancer cells. BMC Cancer. 2010; 10 318-2407-10-318. doi: 10.1186/1471-2407-10-318
17. Lee HS. Mechanisms and consequences of TGF-ss overexpression by podocytes in progressive podocyte disease. Cell Tissue Res. 2012; 347(1):129–140. [PubMed: 21541658]
18. Honkanen E, Teppo AM, Tornroth T, et al. Urinary transforming growth factor-beta 1 in membranous glomerulonephritis. Nephrol Dial Transplant. 1997; 12:2562–2568. [PubMed: 9430852]
19. Hanke N, Staggs L, Schroder P, et al. Zebrafishing for novel genes relevant to the glomerular filtration barrier. Biomed Res Int. 2013; 658270doi: 10.1155/2013/658270
20. Korstanje R, Deutsch K, Bolanos-Palmieri P, et al. Loss of kynurenine 3-mono-oxygenase causes proteinuria. J Am Soc Nephrol. 2016; doi: 10.1681/ASN.2015070835
21. Gbadegesin RA, Hall G, Adeyemo A, et al. Mutations in the gene that encodes the F-actin binding protein anillin cause FSGS. J Am Soc Nephrol. 2014; 25(9):1991–2002. DOI: 10.1681/ASN.2013090976 [PubMed: 24676636]
22. Kreidberg JA, Symons JM. Integrins in kidney development, function, and disease. Am J Physiol Renal Physiol. 279(2):F233–42. 20000. [PubMed: 10919841]
23. Suh JH, Miner JH. The glomerular basement membrane as a barrier to albumin. Nat Rev Nephrol. 2013; 9(8):470–7. DOI: 10.1038/nrneph.2013.109 [PubMed: 23774818]
24. Kruegel J, Rubel D, Gross O. Alport syndrome--insights from basic and clinical research. Nat Rev Nephrol. 2013; 9(3):170–8. DOI: 10.1038/nrneph.2012.259 [PubMed: 23165304]
25. Ghosh S, Singh M, Sahoo R, et al. Alport syndrome: A rare cause of uraemia. BMJ Case Rep. 2014; doi: 10.1136/bcr-2013-201731
26. Zenker M, Aigner T, Wendler O, et al. Human laminin beta2 deficiency causes congenital nephrosis with mesangial sclerosis and distinct eye abnormalities. Hum Mol Genet. 2004; 13(21): 2625–2632. DOI: 10.1093/hmg/ddh284 [PubMed: 15367484]
27. Chen YM, Zhou Y, Go G, et al. Laminin beta2 gene missense mutation produces endoplasmic reticulum stress in podocytes. J Am Soc Nephrol. 2013; 24(8):1223–33. DOI: 10.1681/ASN.2012121149 [PubMed: 23723427]
28. Matejas V, Hinkes B, Alkandari F, et al. Mutations in the human laminin beta2 (LAMB2) gene and the associated phenotypic spectrum. Hum Mutat. 2010; 31(9):992–1002. DOI: 10.1002/humu.21304 [PubMed: 20556798]
29. Zhang YZ, Lee HS. Quantitative changes in the glomerular basement membrane components in human membranous nephropathy. J Pathol. 1997; 183(1):8–15. DOI: 10.1002/(SICI)1096-9896(199709)183:1<8::AID-PATH1079>3.0.CO;2-W [PubMed: 9370941]
30. Girgert R, Martin M, Kruegel J, et al. Integrin alpha2-deficient mice provide insights into specific functions of collagen receptors in the kidney. Fibrogenesis Tissue Repair. 2010; 3:19.doi: 10.1186/1755-1536-3-19 [PubMed: 20860797]
31. Goldberg S, Adair-Kirk TL, Senior RM, et al. Maintenance of glomerular filtration barrier integrity requires laminin alpha5. J Am Soc Nephrol. 2010; 21(4):579–86. DOI: 10.1681/ASN.2009091004 [PubMed: 20150535]
32. Rutnam ZJ, Wight TN, Yang BB. miRNAs regulate expression and function of extracellular matrix molecules. Matrix Biol. 2013; 32(2):74–85. DOI: 10.1016/j.matbio.2012.11.003 [PubMed: 23159731]
33. Williams AE. Functional aspects of animal microRNAs. Cell Mol Life Sci. 2008; 65:545–562. [PubMed: 17965831]
34. Miyazono A, Yamada A, Morimura N, et al. TGF-beta suppresses POEM expression through ERK1/2 and JNK in osteoblasts. FEBS Lett. 2007; 581(27):5321–5326. DOI: 10.1016/j.febslet.2007.10.021 [PubMed: 17977532]

35. Brandenberger R, Schmidt A, Linton J, et al. Identification and characterization of a novel extracellular matrix protein nephronectin that is associated with integrin alpha8beta1 in the embryonic kidney. J Cell Biol. 2001; 154(2):447–458. [PubMed: 11470831]
36. Linton JM, Martin GR, Reichardt LF. The ECM protein nephronectin promotes kidney development via integrin alpha8beta1-mediated stimulation of gdnf expression. Development. 2007; 134(13):2501–2509. [PubMed: 17537792]
37. Miner JH. Mystery solved: Discovery of a novel integrin ligand in the developing kidney. J Cell Biol. 2001; 154(2):257–259. [PubMed: 11470814]
38. Kim JH, Kim BK, Moon KC, et al. Activation of the TGF-beta/Smad signaling pathway in focal segmental glomerulosclerosis. Kidney Int. 2003; 64(5):1715–1721. DOI: 10.1046/j.1523-1755.2003.00288.x [PubMed: 14531804]
39. Kim TS, Kim JY, Hong HK, et al. mRNA expression of glomerular basement membrane proteins and TGF-beta1 in human membranous nephropathy. J Pathol. 1999; 189(3):425–430. DOI: 10.1002/(SICI)1096-9896(199911)189:3<425::AID-PATH454>3.0.CO;2-6 [PubMed: 10547606]
40. Shankland SJ, Pippin J, Pichler RH, et al. Differential expression of transforming growth factor-beta isoforms and receptors in experimental membranous nephropathy. Kidney Int. 1996; 50(1):116–124. [PubMed: 8807580]
41. Yoshioka K, Takemura T, Murakami K, et al. Transforming growth factor-beta protein and mRNA in glomeruli in normal and diseased human kidneys. Lab Invest. 1993; 68(2):154–163. [PubMed: 8441250]
42. Honkanen E, Teppo AM, Tornroth T, et al. Urinary transforming growth factor-beta 1 in membranous glomerulonephritis. Nephrol Dial Transplant. 1997; 12(12):2562–2568. [PubMed: 9430852]
43. Fang L, Kahai S, Yang W, et al. Transforming growth factor-beta inhibits nephronectin-induced osteoblast differentiation. FEBS Lett. 2010; 584(13):2877–2882. DOI: 10.1016/j.febslet.2010.04.074 [PubMed: 20452350]
44. Kimmel CB, Ballard WW, Kimmel SR, et al. Stages of embryonic development of the zebrafish. Dev Dyn. 1995; 203(3):253–310. [PubMed: 8589427]
45. Drummond IA. Zebrafish kidney development. Methods Cell Biol. 2004; 76:501–530. [PubMed: 15602890]
46. Xing Y, Hou J, Guo T, et al. microRNA-378 promotes mesenchymal stem cell survival and vascularization under hypoxic-ischemic conditions in vitro. Stem Cell Res Ther. 2014; 5(6):130.doi: 10.1186/scrt520 [PubMed: 25418617]
47. Kooistra SM, Norgaard LC, Lees MJ, et al. A screen identifies the oncogenic micro-RNA miR-378a-5p as a negative regulator of oncogene-induced senescence. PLoS One. 2014; 9(3):e91034.doi: 10.1371/journal.pone.0091034 [PubMed: 24651706]
48. Feng M, Li Z, Aau M, et al. Myc/miR-378/TOB2/cyclin D1 functional module regulates oncogenic transformation. Oncogene. 2011; 30(19):2242–51. DOI: 10.1038/onc.2010.602 [PubMed: 21242960]
49. Eremina V, Quaggin SE. The role of VEGF-A in glomerular development and function. Curr Opin Nephrol Hypertens. 2004; 13:9–15. [PubMed: 15090854]
50. Nakatani S, Ishimura E, Mori K, et al. Nephronectin expression in glomeruli of renal biopsy specimens from various kidney diseases: nephronectin is expressed in the mesangial matrix expansion of diabetic nephropathy. Nephron Clin Pract. 2012; 122(3-4):114–21. DOI: 10.1159/000350816 [PubMed: 23689482]
51. Nakatani S, Wei M, Ishimura E, et al. Proteome analysis of laser microdissected glomeruli from formalin-fixed paraffin-embedded kidneys of autopsies of diabetic patients: nephronectin is associated with the development of diabetic glomerulosclerosis. Nephrol Dial Transplant. 2012;; 27(5):1889–97. DOI: 10.1093/ndt/gfr682 [PubMed: 22172726]
52. Hentschel DM, Mengel M, Boehme L, et al. Rapid screening of glomerular slit diaphragm integrity in larval zebrafish. Am J Physiol Renal Physiol. 2007; 293(5):F1746–50. DOI: 10.1152/ajprenal.00009.2007 [PubMed: 17699558]

53. Saleem MA, O'Hare MJ, Reiser J, et al. A conditionally immortalized human podocyte cell line demonstrating nephrin and podocin expression. J Am Soc Nephrol. 2002; 13(3):630–638. [PubMed: 11856766]

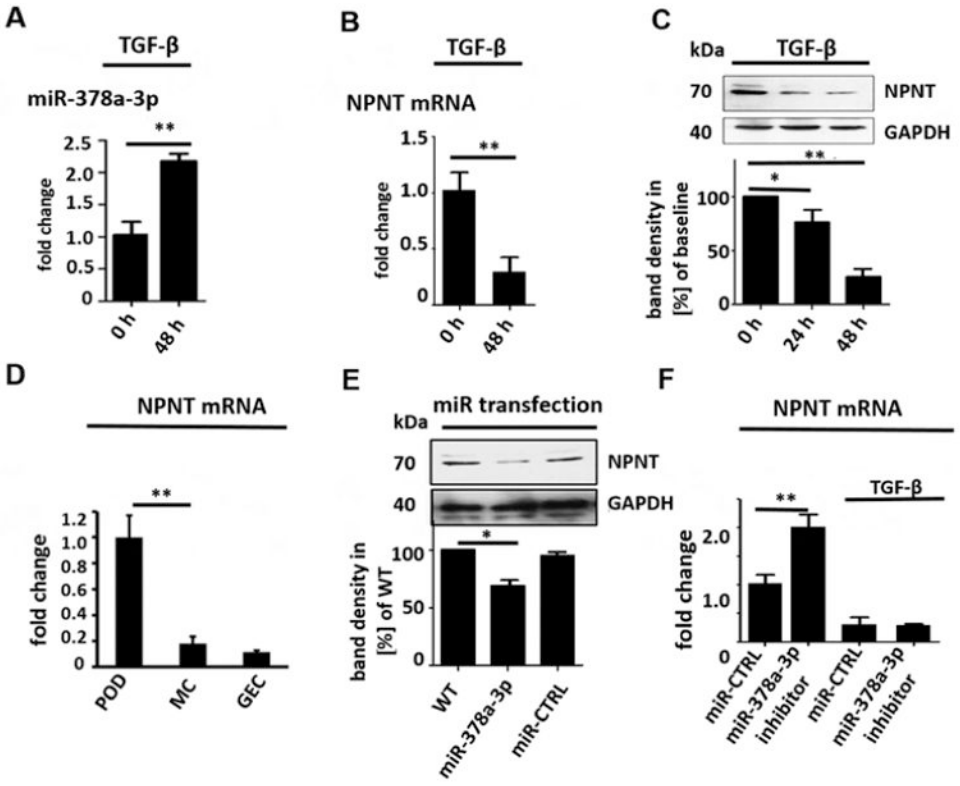

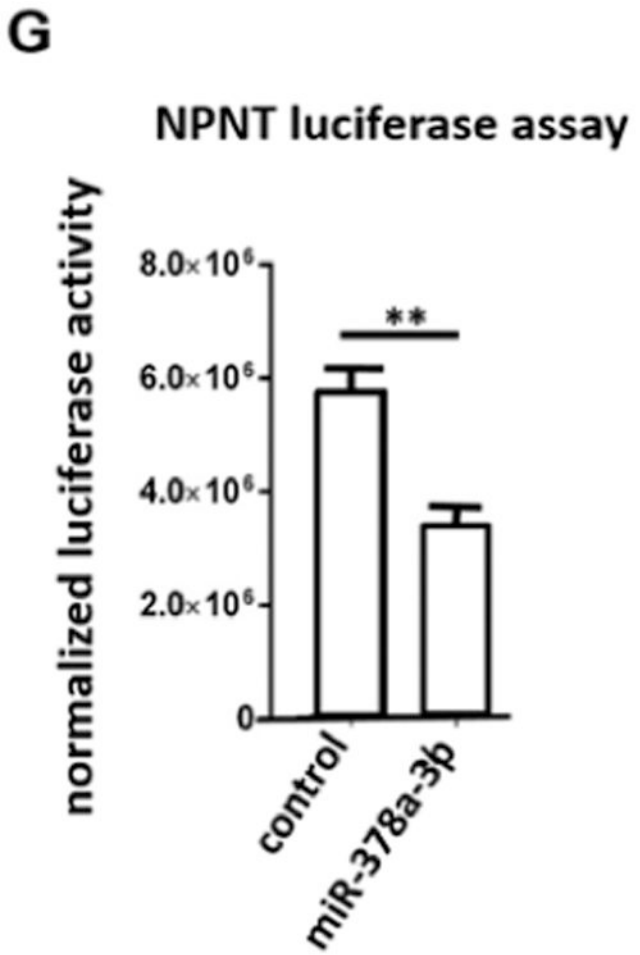

Figure 1. MiR-378a-3p regulates NPNT expression in cultured human podocytes

(A) Real-time PCR reveals induction of miR-378a-3p expression in cultured human podocytes after TGF-β stimulation (5 ng/ml) at 48 h compared to baseline. ** $p<0.01$. (B) Real-time PCR reveals repression of NPNT mRNA in cultured human podocytes after TGF-β stimulation (5 ng/ml) at 48 h compared to baseline. (C) Western blot for NPNT in cultured human podocytes after TGF-β stimulation (5 ng/ml) compared to baseline for the time points indicated. Quantification of NPNT protein expression is given in the histogram. (D) Real-time PCR for relative NPNT mRNA expression in cultured human podocytes (POD), human mesangial cells (MC) and human glomerular endothelial cells (GEC). ** $p<0.01$. (E) Western blot for NPNT in cultured human podocytes at baseline and 72 h after a 4 h transfection with a miR-378a-3p mimic (5 nM) indicates complete suppression of NPNT protein compared to control after 72 h. Quantification of NPNT protein expression is given in the histogram. (F) Real-time PCR reveals upregulation of NPNT in cultured human podocytes after transfection with a miR-378a-3p inhibitor. Stimulation with TGF-β in the presence of a miR-378a-3p inhibitor decreased NPNT expression comparable to stimulation with TGF-β alone. ** $p<0.01$. (G) Luciferase reporter assay to validate miR-378a-3p binding to NPNT was performed in human embryonic kidney cells 293 (HEK cells). Cells were lysed 24 h after transfection and subsequently used for luciferase activity. Luciferase reads were normalized with beta-Gal values. ** $p<0.01$.

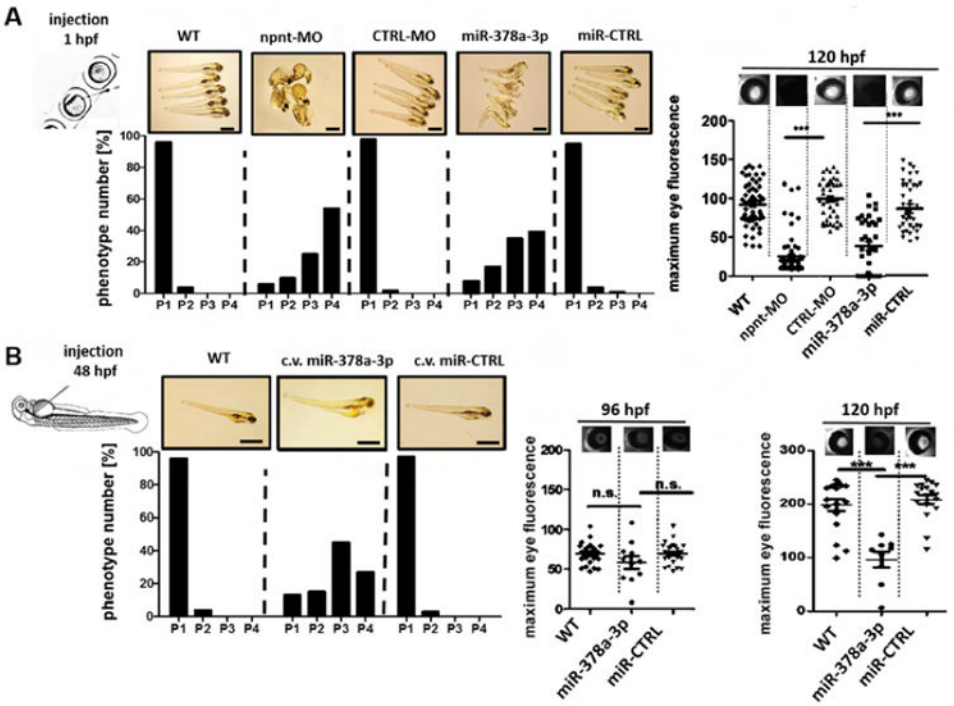

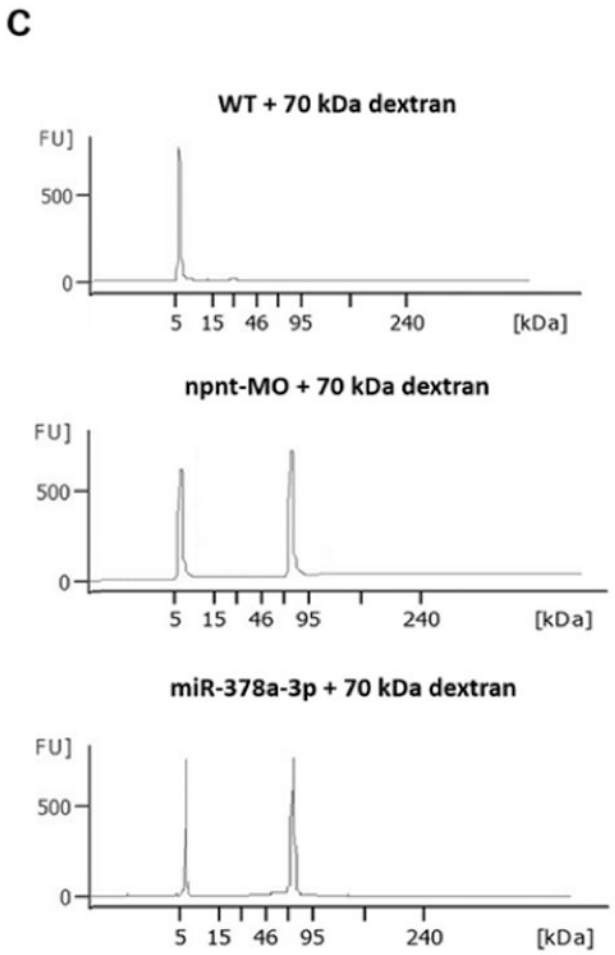

Figure 2. Npnt knockdown by morpholino or injection of miR-378a-3p in zebrafish larvae induces edema and proteinuria

(A). Quantification of edemous phenotype (left panel) and loss of circulating high molecular weight proteins by measuring max. eye fluorescence in the retinal vessel plexus of Tg(l-fabp:DBP:EGFP) zebrafish (right panels) at 120 hours post fertilization (hpf). Zebrafish were injected with a npnt specific morpholino (npnt-MO (100 μM)), a scrambled control morpholino (CTRL-MO (100 μM)), a miR-378a-3p mimic (25 μM) or a miR-CTRL (25 μM) at 1 hpf compared to uninjected wildtype animals (WT). Scale bar = 500 μm.

(B). Quantification of edemous phenotype (left panel) and loss of circulating high molecular weight proteins by measuring max. eye fluorescence in the retinal vessel plexus of Tg(l-fabp:DBP:EGFP) zebrafish (right panels) at 96 hpf and 120 hours post fertilization (hpf). Zebrafish larvae were injected with a miR-378a-3p mimic (25 μM) or a miR-CTRL (25 μM) in the cardinal vein (c.v.) at 48 hpf compared to WT condition. The edemous phenotype of the larvae was categorized in 4 groups: P1 = no edema, P2 = mild edema, P3 = severe edema, P4 = very severe edema. Fluorescent images of the retinal vessel plexus of Tg(l-fabp:DBP:EGFP) zebrafish larvae at 96 hpf injected with morpholinos or miRNAs as indicated. Graph represents maximum fluorescence intensity detected in the fish eye. *** $p<0.001$, n.s. not significant. Scale bar = 500 μm.

(C). Zebrafish water after injection of a red fluorescent 70 kDa dextran in npnt-MO (100 μM) or miR-378a-3p mimic (25 μM) treated zebrafish larvae was analysed by protein on chip electrophoresis. The first peaks represents 5 kDa marker peak, second peak represents detected 70 kD dextran. Each sample consisted of pooled medium from 10 fish kept in 200 μl embryo raising medium for 48 h.

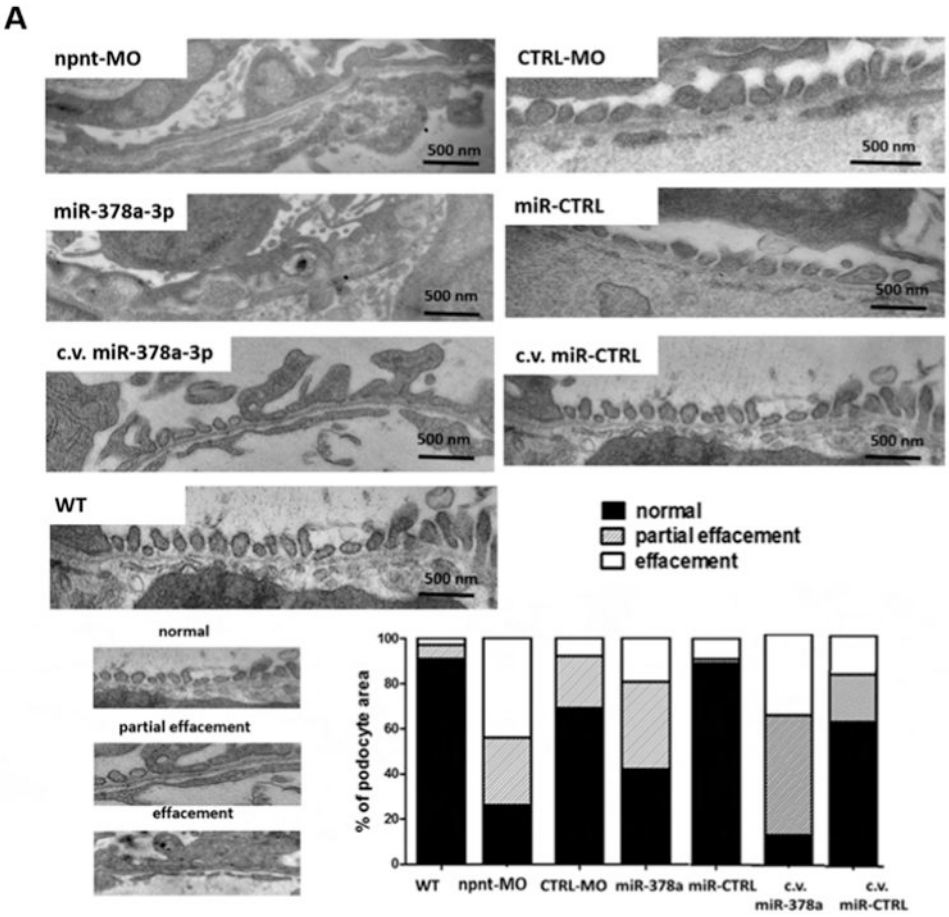

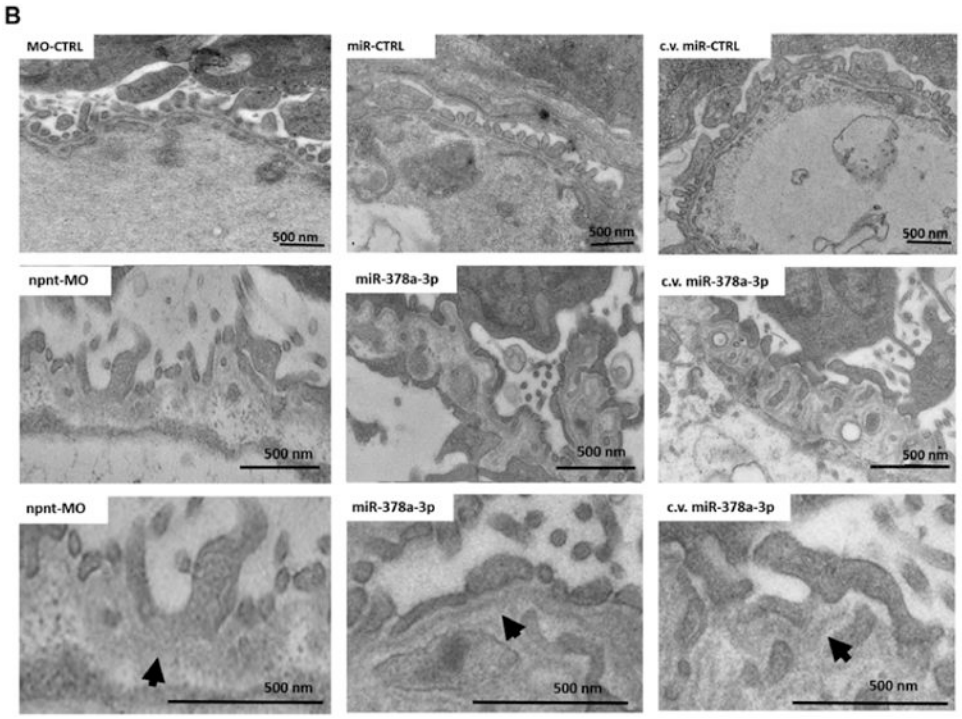

Figure 3. Ultrastructural changes of the glomerulus after npnt knockdown by morpholino or miR-378a-3p in zebrafish larvae

Transmission electron microscopy pictures and quantification of podocyte effacement (A) and widening of the lamina rara interna of the GBM (B) in zebrafish larvae 120 hpf. Normal, partial and complete effacement of podocytes is compared between WT zebrafish and zebrafish that were injected with npnt-MO (100 μM), CTRL-MO (100 μM), miR-378a-3p mimic (25 μM) or miR-CTRL (25 μM) in one to four cell stage or in the cardinal vein of the zebrafish at 48 hpf (c.v. miR-378a-3p (25 μM), c.v. miR-CTRL (25 μM)). Podocyte layer was analysed over a length of 91 μm for WT, 98 μm for miR-378a-3p, 86 μm for miR-CTRL, 104 μm for npnt-MO, 80 μm for CTRL-MO, 78 μm for c.v. miR-378a-3p and 84 μm for c.v. miR-CTRL. Scale bar = 500 nm.

C.v.: cardinal vein injection at 48 hpf; hpf: hours post fertilization. Bars indicate quantification of results.

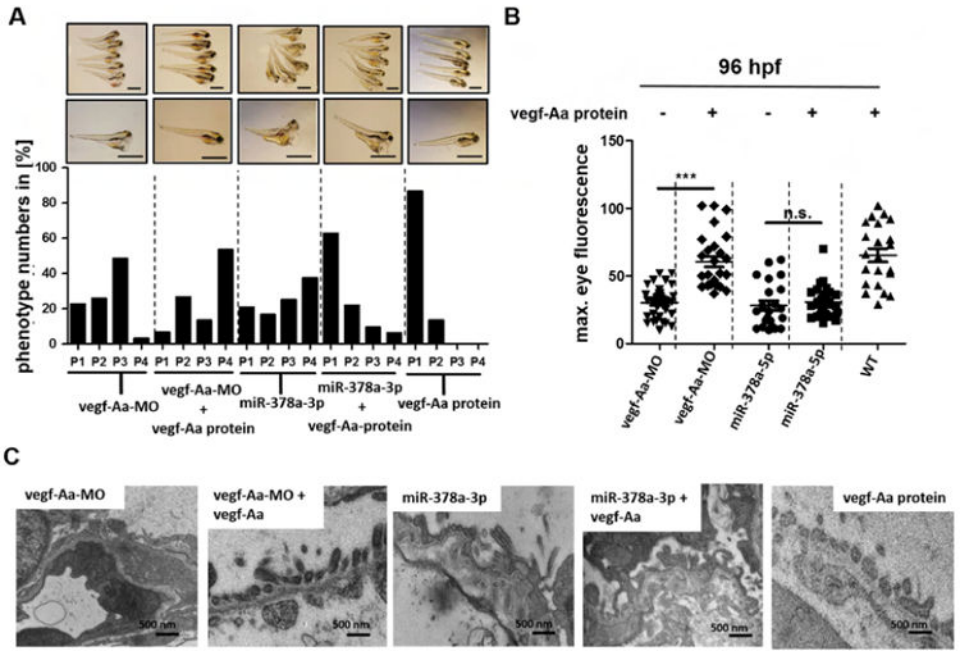

Figure 4. Vegf-Aa does not rescue miR-378a-3p induced glomerular damage in zebrafish larvae

Zebrafish larvae were injected with vegf-Aa-MO (100 μM), miR-378a-3p mimic (25 μM) or co-injected with either vegf-Aa MO (150 μM) and vegf-Aa zebrafish protein (2.5 nl of 250 ng/ml solution) or miR-378a-3p mimic (25 μM) and a vegf-Aa zebrafish protein (2.5 nl of 250 ng/ml solution) at one to four cell stage. Scale bar = 500 μm.

(A) The phenotype of the larvae was categorized into 4 groups: P1 = no edema, P2 = mild edema, P3 = severe edema, P4 = very severe edema depending on yolk sack. Scale bar = 500 μm. (B) Quantification of loss of circulating high molecular weight proteins by measuring max. eye fluorescence in the retinal vessel plexus of Tg(l-fabp:DBP:EGFP) zebrafish. Scatter plot graph presenting maximum fluorescence intensity of the fish eye was analysed with image J.

(C) Transmission electron microscopy pictures of zebrafish at 120 hpf. Swelling of glomerular endothelium after vegf-Aa-MO injection and thickening of the GBM together with podocyte effacement after miR-378a-3p mimic and after miR-378a-3p mimic/ vegf-Aa protein co-injection is illustrated. Scale bar = 500 nm.

*** $p<0.001$, n.s. not significant; hpf: hours post fertilisation.

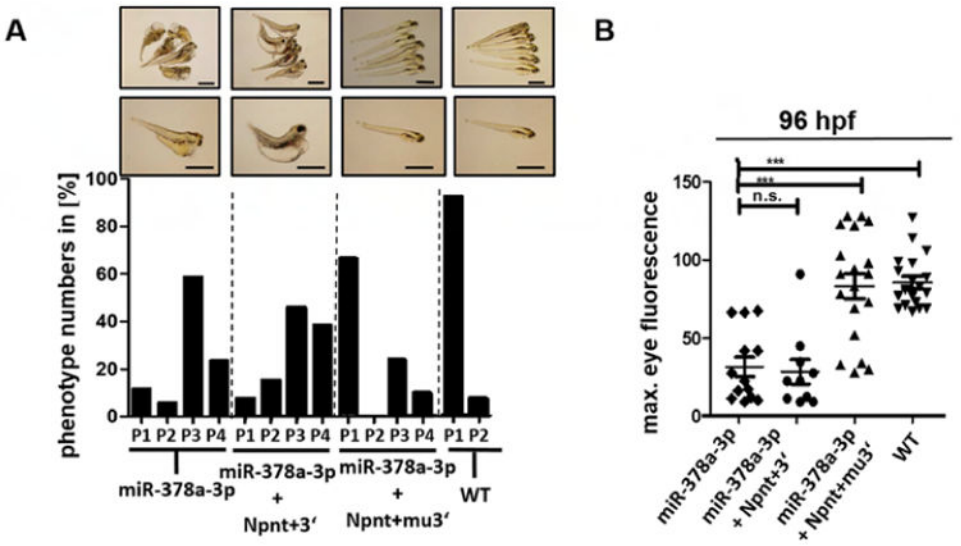

Figure 5. Transspecies npnt rescue with different mice Npnt constructs after miR-378a-3p overexpression

(A) Phenotype development in zebrafish larvae at 120 hpf. Zebrafish were injected with a miR-378a-3p mimic (miR-378a-3p), miR-378a-3p mimic and cRNA of mouse Npnt+3′ construct (miR-378a-3p+ Npnt+3′) or miR-378a-3p mimic and cRNA of mouse Npnt +3′construct (miR-378a-3p + Npnt+mu3′). The phenotype of the larvae was categorized in 4 groups: P1 = no edema, P2 = mild edema, P3 = severe edema, P4 = very severe edema. Scale bar = 500 μm. (B) Loss of circulating high molecular weight proteins in zebrafish larvae at 120 hpf. Zebrafish were injected with a miR-378a-3p mimic (miR-378a-3p), miR-378a-3p mimic and cRNA of mouse Npnt+3′ construct (miR-378a-3p + Npnt+3′), or miR-378a-3p mimic and cRNA of mouse Npnt+mu3′construct (miR-378a-3p + Npnt +mu3′). Graph represents maximum fluorescence intensity detected in the fish eye. *** $p<0.001$, n.s. not significant.

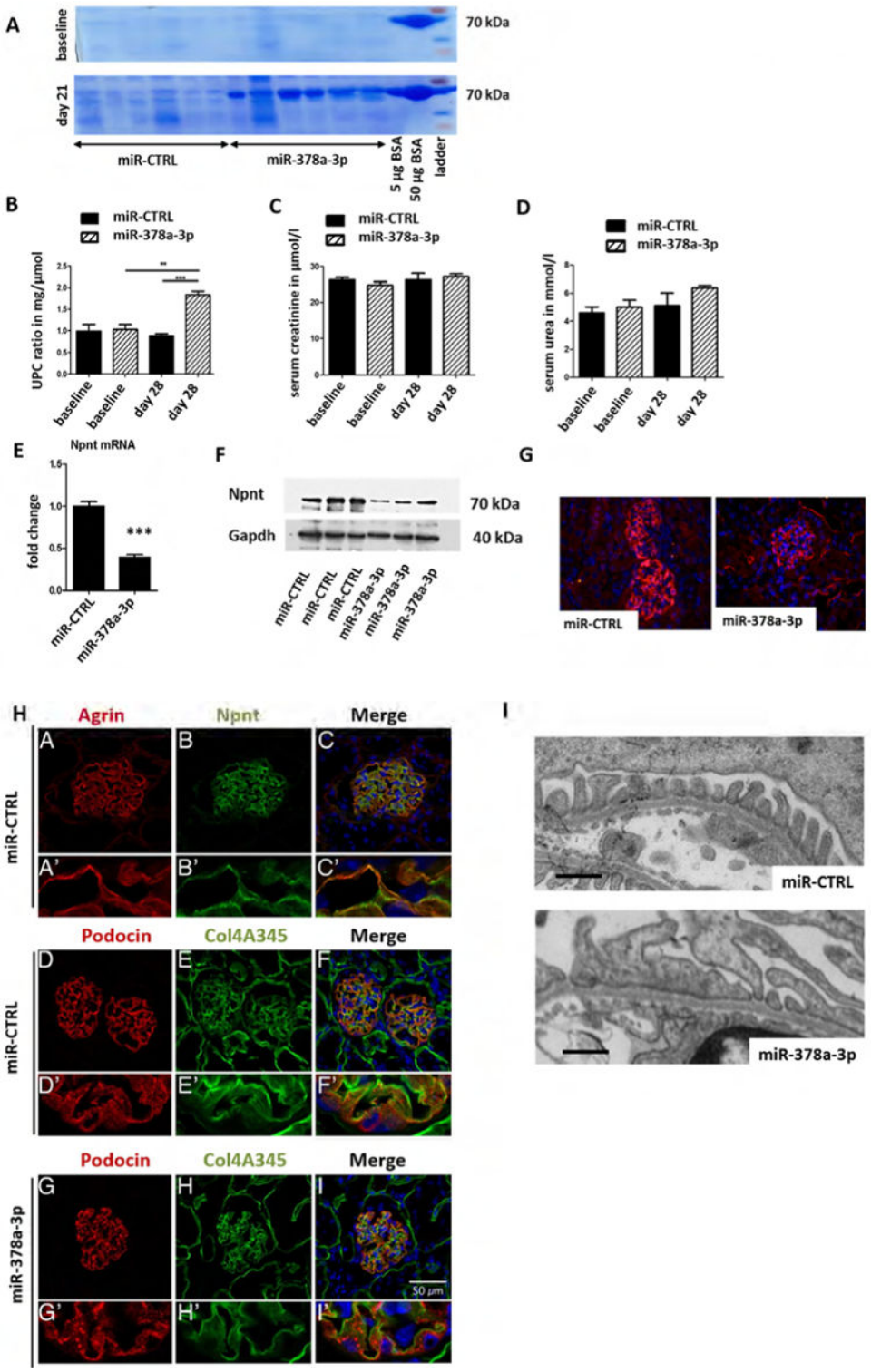

Figure 6. MiR-378a-3p mimic injection leads to albuminuria, podocyte effacement and altered expression of podocin in mice

Mice were either injected with a miR-CTRL (0.2 mg/ mouse) or a miR-378a-3p mimic (0.2 mg/mouse) at day 0, 3, 7 and 14. n = 12.

(A) Coomassie gel from urine samples of mice injected with either miR-CTRL or miR-378a-3p mimic at baseline and 28 days after the first injection. 5 μg and 50 μg BSA were also run on both gels. BSA: bovine serum albumin. UPC-ratio (B), serum creatinine (C) and serum urea (D) of miR-CTRL and miR-378a-3p mimic injected mice at baseline and 28 days after the first injection. ** $p< 0.01$, *** $p< 0.001$. Measurements were performed with OLYMPUS. Differences in serum creatinine and serum urea were not significant.
(E) Real-time PCR for Npnt mRNA expression in whole kidney sections of mice injected with either miR-CTRL or miR-378a-3p mimic at baseline and 28 days after the first injection.
(F) Western blot of whole kidney sections of mice injected with either miR-CTRL or miR-378a-3pmimic at baseline and 28 days after the first injection. Western blot bands were normalised to Gapdh.
(G) Immunofluorescent staining for Npnt (red) and DAPI nuclear staining (blue) on paraffin sections of glomeruli from miR-CTRL (0.2 mg/ mouse) and miR-378a-3p mimic (0.2 mg/ mouse) injected mice.
(H) Immunofluorescent staining for agrin (red, A, A′) and Npnt (green, B, B′) on cryo sections of glomeruli from miR-CTRL injected mice. The merged picture (C, C′) shows a partial overlap of agrin and Npnt in the GBM in orange. Immunofluorescence staining for podocin (red D, D′, G, G′) and collagen 4A345 (green E, E′, H, H′) on cryo sections of glomeruli from mice injected with miR-CTRL (0.2 mg/ mouse, D-F) or miR-378a-3p mimic (0.2 mg/ mouse G-I). F, F′, I and I′ show the merged pictures. Podocin staining shows a speckled pattern in miR-378a-3p mimic injected mice. Scale bar = 50 μm.
(I) Transmission electron microscopy pictures of glomeruli from mice injected with miR-CTRL (0.2 mg/ mouse) or miR-378a-3p mimic (0.2 mg/ mouse) at day 0, 3, 7 and 14. MiR-378a-3p injected mice develop podocyte effacement. Scale bar = 500 nm.

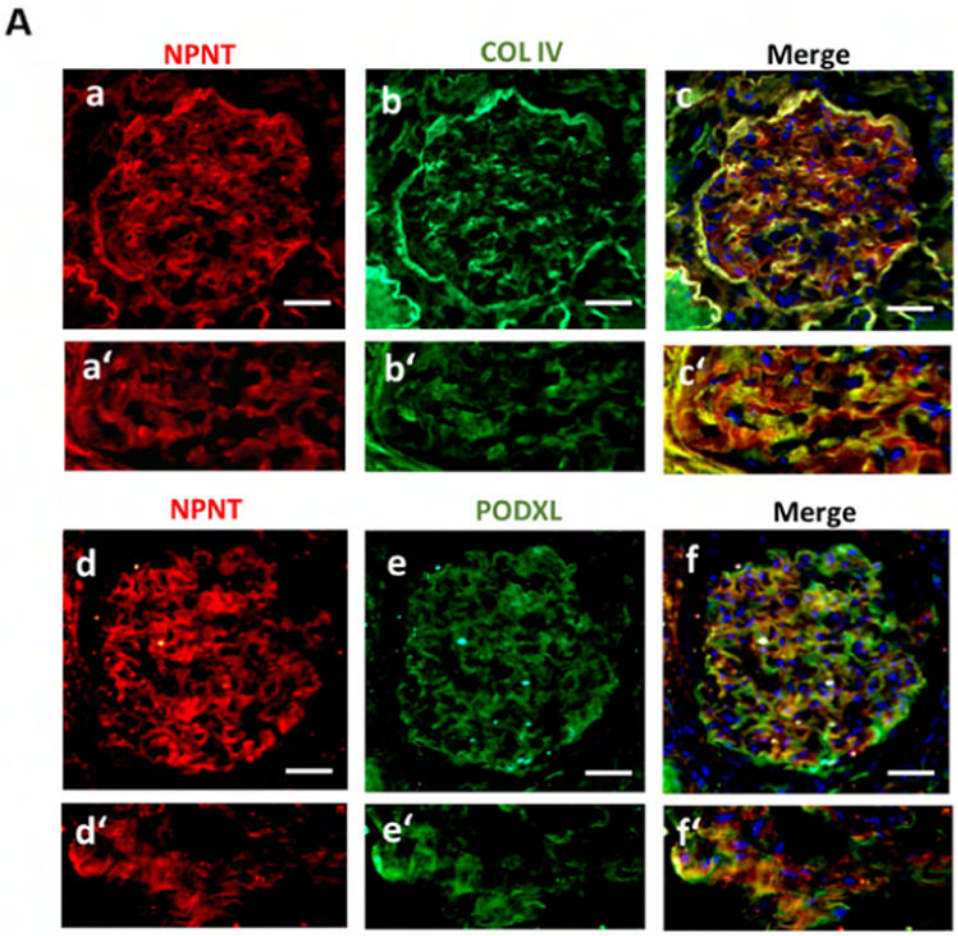

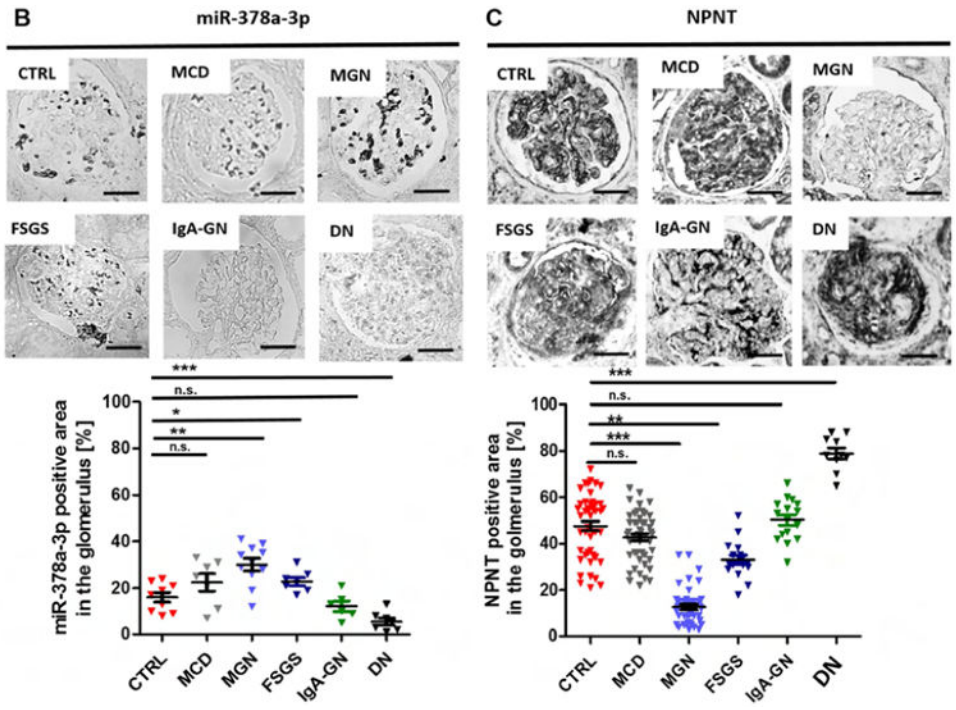

Figure 7. Expression of miR-378a-3p and NPNT in glomerular diseases

(A) Immunofluorescence double staining for NPNT (red; a, a′) and collagen IV (green; b, b′) as well as NPNT (red; d, d′) and podocalyxin (PODXL, green; e, e′) on human nephrectomy. Overlaps of both staining are shown in the merged pictures in yellow (c, c′, f, f′); scale bar = 50 μm.

In situ hybridization for miR-378a-3p (B) and immunohistochemistry staining for NPNT (C) on kidney biopsies from patients with different glomerular diseases. The lower panels depict quantification of miR-378a-3p and NPNT-positive area. Each triangle represents analysis of one glomerulus. * $p < 0.05$, ** $p < 0.01$, *** $p < 0.001$, n.s. not significant. Scale bar = 50 μm.